

# Physical aging of ultrathin glassy polymer films tracked by gas permeability

Brandon W. Rowe, Benny D. Freeman, Donald R. Paul\*

Department of Chemical Engineering, Texas Materials Institute and Center for Energy and Environmental Resources, The University of Texas at Austin, Austin, Texas 78712, United States, USA

## ARTICLE INFO

### Article history:

Received 10 July 2009

Received in revised form

7 September 2009

Accepted 13 September 2009

Available online 1 October 2009

### Keywords:

Physical aging

Gas permeability

Membranes

## ABSTRACT

Membrane-based separations play a key role in energy conservation and reducing greenhouse gas emissions by providing low energy routes for a wide variety of industrially-important separations. For reasons not completely understood, membrane permeability changes with time, due to physical aging, and the rate of permeability change can become orders of magnitude faster in films thinner than one micron. The gas transport properties and physical aging behavior of free-standing glassy polysulfone and Matrimid® films as thin as 18 nm are presented. Physical aging persists in glassy films approaching the length scale of individual polymer coils. The films studied ranged from 18–550 nm thick. They exhibited reductions in gas permeability, some more than 50%, after ~1000 h of aging at 35 °C, and increases in selectivity. The properties of these ultrathin films deviate dramatically from bulk behavior, and the nature of these deviations is consistent with enhanced mobility and reduced  $T_g$  in ultrathin films. The Struik physical aging model was extended to account for the influence of film thickness on aging rate, and it was shown to adequately describe the aging data.

© 2009 Elsevier Ltd. All rights reserved.

## 1. Introduction

The multitude of thin polymer film applications in, for example, microelectronics, coatings, separations, and optics, has stimulated great interest in understanding polymer properties at the nanoscale [1–8]. Behavior of the glass transition temperature,  $T_g$ , (which is typically associated with long-range cooperative molecular motion and is often referred to as the softening point of a rigid, amorphous glassy polymer) in ultrathin polymer films is an area of intensive research and debate [3,9–14]. Typically, as film thickness decreases, free standing films and films supported on non-attractive substrates exhibit decreasing  $T_g$ , while films on attractive substrates show increasing  $T_g$  [13]. These deviations from bulk behavior are generally attributed to enhanced mobility at the free surface and attractive substrate-polymer interactions, respectively [3,13]. However, the genesis of these property changes is not completely understood because different experimental techniques can reveal apparently conflicting results, such as the divergent thickness-dependence of the dilatometric and dielectric  $T_g$  of hyperbranched polyesters reported by Serghei et al. [12,14]. Additionally, Forrest et al. have shown that the same polystyrene samples which exhibit decreasing  $T_g$  with film thickness, indicating that molecular motion is faster in thinner films, also show an increase in the time constant for

interfacial healing, which would typically suggest that molecular motion of the polymer chain segments is slower in thinner films [14]. Clearly, many questions remain to fully understand the fascinating, complex dynamics of ultrathin, highly confined glassy polymers.

While the influence of film thickness on  $T_g$  has been an active area of scientific study, much less effort has focused on the influence of ultrathin-film confinement effects on physical aging in glassy polymers [9,15–17]. Physical aging arises from the inherent non-equilibrium nature of glassy polymers and causes material properties to drift over time towards a seemingly unattainable equilibrium [18–20]. The effects of physical aging are thermo-reversible, i.e., changes caused by physical aging can be erased by heating above the glass transition. Thin film glassy polymers are used, or proposed for use, in a wide variety of important technological applications (e.g., gas and liquid separation membranes, fuel cells, solar cells, lithography, and optical materials) [6,7,21–23], and the performance of these thin films over time can significantly influence end-use properties (e.g., gas flux through ultrathin membranes used for gas separations) [24], so it is critical to enhance the fundamental understanding of physical aging in thin films. Polystyrene films as thin as 18 nm undergo physical aging, as evidenced by a volumetric overshoot upon heating in ellipsometry measurements; however, no information regarding the extent or rate of aging in such thin films has been reported [16]. The fluorescence intensity of chromophore-labeled poly(isobutyl methacrylate) films as thin as 10 nm have been studied as a function of aging; however, a thickness dependent aging rate was not clearly observed [9]. Similar work by

\* Corresponding author. Tel.: +1 512 471 5392; fax: +1 512 471 0542.  
E-mail address: [drp@che.utexas.edu](mailto:drp@che.utexas.edu) (D.R. Paul).

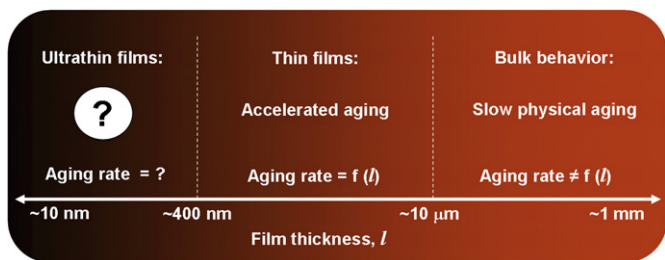


Fig. 1. Schematic defining length scales of interest.

Priestley et al. have shown reduced aging rates in supported 20 nm poly(methyl methacrylate) films as compared to 500 nm films [25]. The reduced aging rate was attributed to attractive interactions between the polymer and silicon substrate restricting polymer chain mobility.

As a first step towards understanding the aging behavior of gas separation membranes, which have a complex, asymmetric hollow fiber structure produced via phase inversion processes, [26] well-defined free-standing films of known thickness in the relevant thickness range were studied. Relative to bulk (i.e., thick film) behavior, gas permeability exhibits dramatically faster physical aging in free-standing glassy polymer films as thin as 400 nm thick [24,27–29]. However, to give high productivity, the selective layer of modern gas separation membranes is on the order of 50–100 nm thick, and it has not been clear, until now, how aging behavior evolves with thickness below 400 nm, especially when approaching length scales similar to that of the polymer coil size [23]. Fig. 1 characterizes the relevant thickness ranges and the general knowledge about physical aging in each regime. Studies of physical aging in ultrathin films should provide insight regarding the mechanisms which cause accelerated aging in thin films and yield a better understanding of the influence of free surfaces and confinement on polymer films. Moreover, such information would be of fundamental importance in developing predictive models of the long-term permeation properties of gas separation membranes.

This study presents the gas permeability and physical aging behavior of polysulfone (PSF) and Matrimid® films as thin as 18 nm. Large deviations from bulk behavior were observed and are discussed in relation to the influence of the free surface on polymer mobility. The physical aging model developed by Struik is extended to include the influence of film thickness and accurately describes the observed aging behavior. The results of this study are consistent with the notion of enhanced mobility at the polymer/air interface.

## 2. Experimental

Bisphenol A-based polysulfone (PSF) from Solvay Advanced Polymers (UDEL PSF-3500 NT LCD) and the polyimide commercially known as Matrimid® 5218 from Huntsman Advanced Materials were used as received in this study. PSF and Matrimid® were chosen because they are widely used gas separation membrane materials, and they have  $T_g$ s (186 °C and 317 °C, respectively) well above the temperature of use (approximately ambient in many cases), so they are deep within the glassy state during use [23,24]. Thin polymer films were prepared by spin casting solutions of the polymers in cyclopentanone onto silicon wafers at 1000 rpm for 60 s; film thickness was controlled by varying the solution concentration. A variable angle spectroscopic ellipsometer manufactured by J.A. Woollam Co., model 2000D, was used to measure film thickness.

A major roadblock to studying gas permeability in ultrathin films is the presence of microscopic pinhole defects, which form with increasing frequency as film thickness is reduced [4]. While

this issue may have little influence on results from studies using ellipsometry, fluorescence spectroscopy, and other techniques, these trans-membrane defects destroy selectivity and mask permeability of a material under study, thereby rendering the sample useless for gas transport studies. Indeed, a defect fraction of  $10^{-6}$  on an area basis is enough to prevent a membrane from performing a gas separation [30]. A coating technique has been applied to circumvent this problem. After spin-coating an ultrathin glassy film of amorphous PSF or Matrimid®, a thin layer of highly permeable, rubbery poly(dimethylsiloxane) (PDMS) was coated directly on top of the glassy film. The PDMS overcoat was created by spin casting a PDMS solution in cyclohexane directly on the glassy film supported on a silicon wafer. The PDMS solution consisted of Dehesive 940A with a proprietary crosslinker (V24) and catalyst (OL) system provided by Wacker Silicones Corporation, Adrian, MI; cyclohexane was added to create a 12 wt.% silicon solution. The film was then annealed at 110 °C for 15 min to crosslink the PDMS and remove residual solvent. Fig. 2 presents a cartoon of the structure of the films used in this study. The thickness of the PDMS layer was measured using a Dektak 6 M stylus profilometer. The PDMS layer effectively blocks convective flow through any pinhole defects of the glassy layer and, at ambient conditions, PDMS is more than 150 °C above its  $T_g$ , so it does not undergo physical aging; consequently, its properties do not change with time [27]. Historically, the development of a similar coating technique for hollow fiber membranes initially enabled the industrial development of these materials for gas separation [30,31]. However, until now, this approach has never been harnessed to study physical aging, as probed via gas permeability, in ultrathin (i.e., <100 nm) films. The two layer film was then lifted from the silicon support using a thin metal wire frame and heated 15 °C above the bulk  $T_g$  of the glassy layer for 20 min to erase the thermal history and define a starting point for the aging studies. The sample preparation techniques are based on those described for single layer films by Huang and Paul [24].

The gas permeability coefficients of the films were measured using a standard constant volume, variable pressure method [32]. Measurements were conducted at 35 °C, an upstream pressure of 2 atm and a maximum downstream pressure of 10 Torr. When not being tested, samples were aged in a dry environment at 35 °C.

## 3. Results and discussion

### 3.1. Influence of PDMS coating on gas transport and aging behavior

The mass transfer resistance from the PDMS layer, which is constant with time, [27] is significantly less than that from the glassy layer due to the much higher gas permeability of PDMS than PSF and Matrimid®, and it can be accounted for using the following resistance model, allowing one to access the native properties of the glassy film: [33]

$$\frac{l_{\text{composite}}}{P_{\text{composite}}} = \frac{l_{\text{PDMS}}}{P_{\text{PDMS}}} + \frac{l_{\text{Glassy}}}{P_{\text{Glassy}}} \quad (1)$$

where  $l_{\text{PDMS}}$  and  $l_{\text{Glassy}}$  are the thicknesses of the PDMS and glassy polymer (i.e., PSF or Matrimid®) layers, respectively;  $P_{\text{PDMS}}$  and

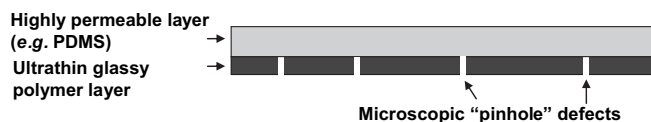
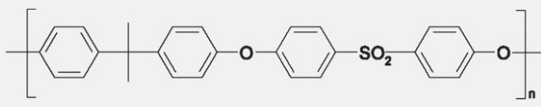
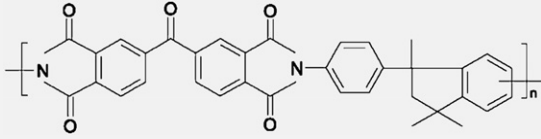
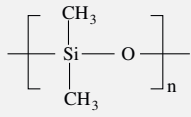


Fig. 2. Diagram of film structure used in this study (not to scale).

**Table 1**  
Bulk material properties.

Polymer	$T_g$	$P_{O_2}$	$P_{N_2}$	$P_{CH_4}$
 Polysulfone	186 °C	1.4	0.24	0.29
 Matrimid®	317 °C	2.12	0.32	0.28
 Poly(dimethylsiloxane)	-123 °C	800	400	1200

Permeability values are given in Barrers; 1 Barrer =  $1 \times 10^{-10}$  [cm<sup>3</sup>(STP) cm/(cm<sup>2</sup> sec cmHg)].

$P_{\text{Glassy}}$  are the permeability coefficients of the PDMS and glassy polymer, respectively. The total thickness of the composite structure (i.e., the glassy polymer overcoated with PDMS) is  $l_{\text{composite}} = l_{\text{PDMS}} + l_{\text{Glassy}}$ , and the permeability of the composite structure is  $P_{\text{composite}}$ . By measuring the thickness of each layer and knowing the PDMS permeability, Equation (1) can be used to calculate the permeability of the glassy polymer layer from permeability measurements on the composite structure.

The structure, glass transition temperature, and bulk permeability of the polymers of interest are recorded in Table 1 [24,34,35]. The PDMS layer was typically 3–4  $\mu\text{m}$  thick. In the thicker films studied in this work (>100 nm), the mass transfer resistance from the PDMS layer was only a few percent or less of the resistance due to the glassy layer. In the thinnest films studied ( $\sim 20$  nm), the contribution from PDMS was  $\sim 20\%$  of the total mass transfer resistance.

The PDMS layer is not strongly adhered to the glassy film; it is easily separated from the glassy layer, so the PDMS layer should not

significantly influence the behavior of the underlying glassy polymer. To investigate any influence the PDMS coating might have on the aging response of these glassy films, the aging behavior of PSF films of similar thicknesses with and without a PDMS coating is shown in Fig. 3. The error bars in this figure represent the average standard deviation for permeability measurements of three different films of each case. The aging behavior of a 465 nm film prepared by coating PSF with a thin PDMS layer is identical, within experimental error, to that of a PSF film of similar thickness but without a PDMS coating, so the presence of the PDMS layer does not perceptibly alter the aging response.

### 3.2. Gas permeability and aging in PSF films

Figs. 4a, b, and c show the oxygen, nitrogen, and methane permeability, respectively, as a function of aging time for PSF films with thicknesses ranging from 465 nm down to 20 nm. The “bulk” aging response of a 60  $\mu\text{m}$  thick film is included for comparison. The films were aged at 35 °C in a dry environment between measurements. Despite being 150 °C below the bulk  $T_g$  of PSF, dramatic aging effects on permeability are evident in the ultrathin films. The gas permeability rapidly decreases with aging time in all films as the material evolves towards the more dense, equilibrium state, and the permeability for most of the thin films is less than that of the bulk PSF. The permeability of these films decreases to  $\sim 50\%$  of the initial value after 1000 h, significantly more than the 10% decrease reported for bulk-like films at similar aging times [24]. The higher permeability of these films, as compared to the bulk oxygen permeability of 1.4 Barrer reported by McHattie et al. [34], for instance, is believed to result from the rapid quench from above  $T_g$ , which captures additional free volume in the polymer. Differences in reported permeabilities for glassy polymers are common, because gas transport properties depend strongly on the thermal history of a glassy polymer [36].

The  $O_2/N_2$  and  $O_2/CH_4$  pure gas selectivity as a function of aging time for each PSF film studied is shown in Fig. 5a and b, respectively; the bulk aging response is shown for comparison. The selectivity in all films is near or above the bulk value, so the ultrathin films behave as effectively defect-free films. The  $O_2/N_2$  and  $O_2/CH_4$  selectivity increases as the material ages; the polymer densification accompanying physical aging reduces the free volume of the polymer

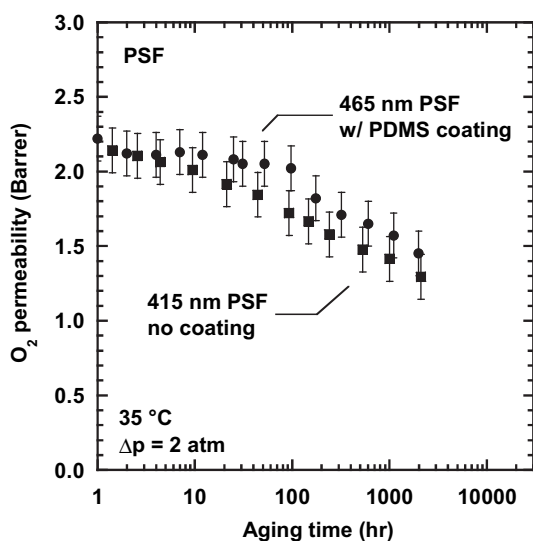


Fig. 3. Comparison of PSF aging behavior with and without PDMS coating.

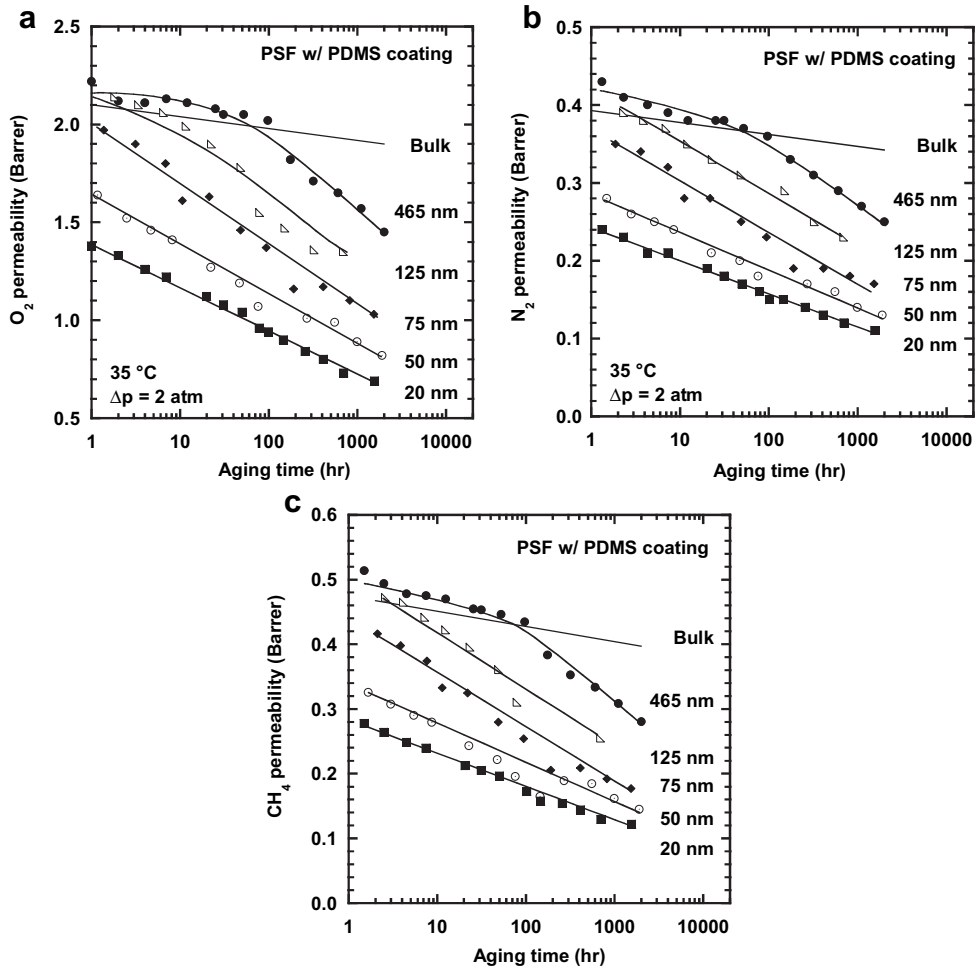


Fig. 4. Influence of physical aging on oxygen permeability (a), nitrogen permeability (b), and methane permeability (c) in PSF films ranging from 465 nm to 20 nm in thickness. Lines are provided to guide the eye.

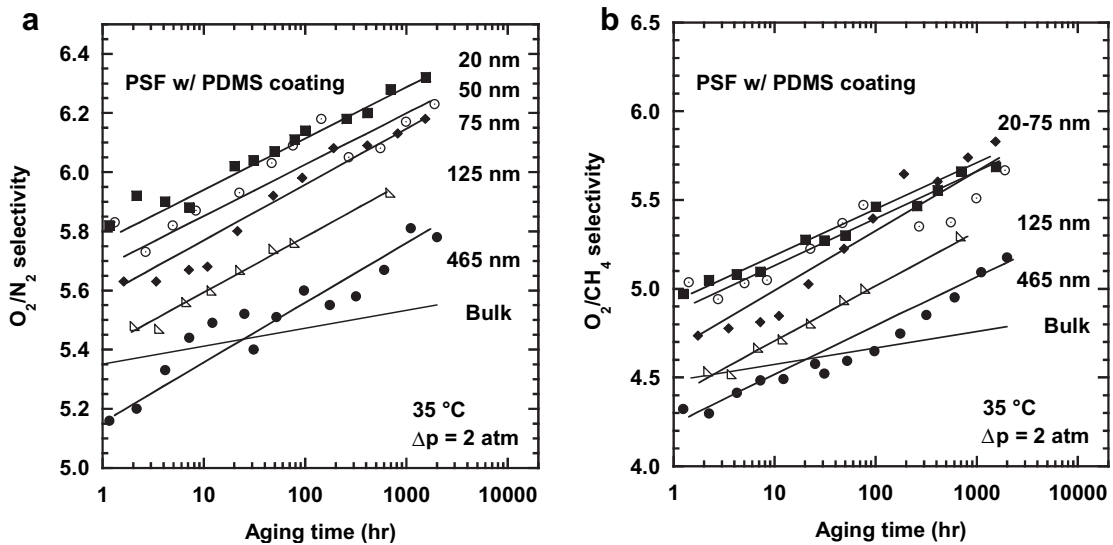
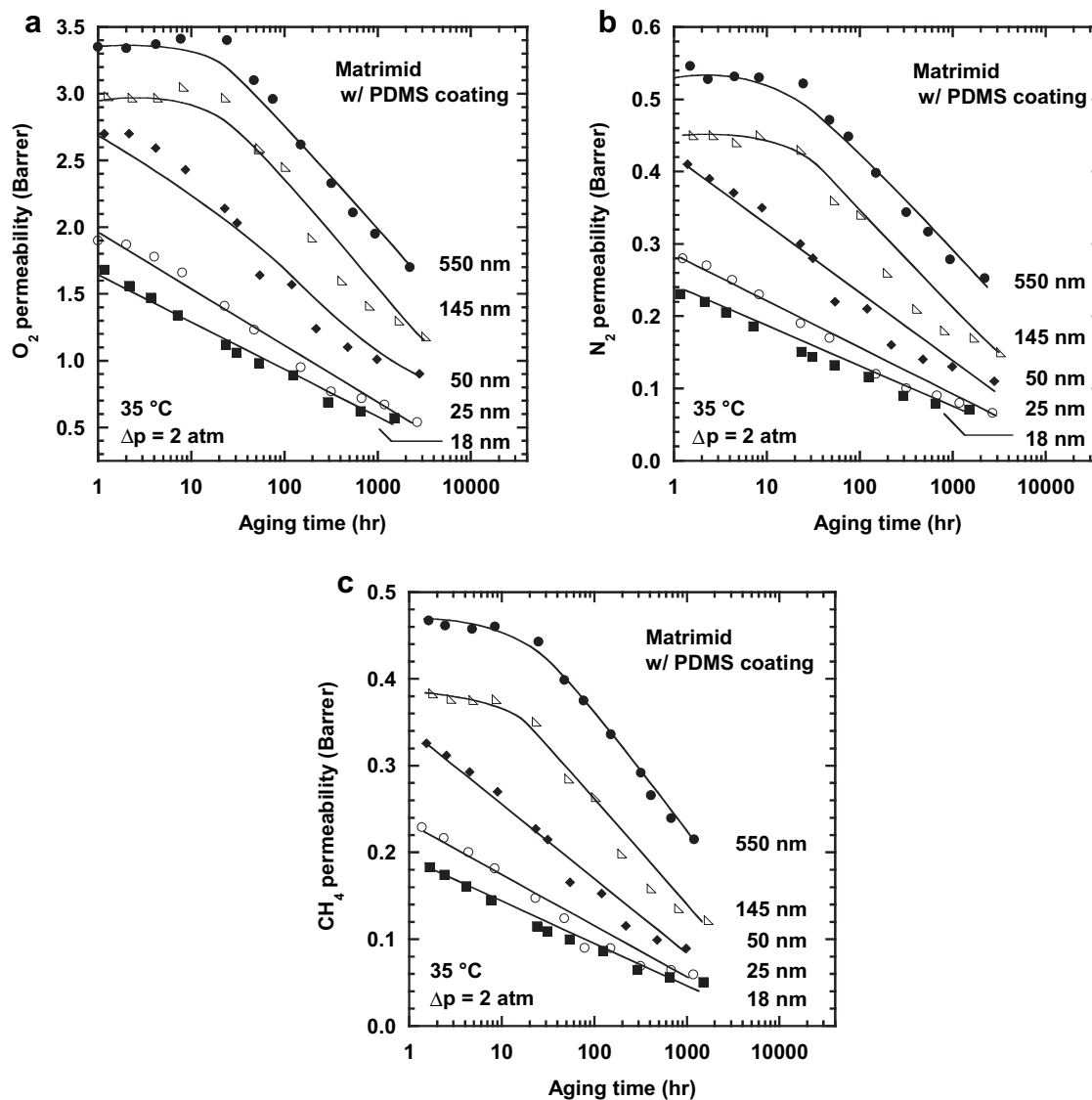


Fig. 5. Influence of physical aging on O<sub>2</sub>/N<sub>2</sub> pure gas selectivity (a) and O<sub>2</sub>/CH<sub>4</sub> pure gas selectivity (b) in PSF films ranging from 465 nm to 20 nm in thickness as a function of aging time. Lines are provided to guide the eye.



**Fig. 6.** Influence of physical aging on oxygen permeability (a), nitrogen permeability (b), and methane permeability (c) in Matrimid<sup>®</sup> films ranging from 550 nm to 18 nm in thickness. Lines are provided to guide the eye.

which, in turn, makes the material more size selective by reducing the diffusion of the larger N<sub>2</sub> and CH<sub>4</sub> molecules more than that of smaller O<sub>2</sub> molecules [24]. The N<sub>2</sub>/CH<sub>4</sub> selectivity also increases with physical aging of PSF (e.g., from 0.85 to 0.90 in the 20 nm film after 1000 h); however these small changes led to more scatter of the data and are not shown for brevity.

Interestingly, the initial permeability, at 1 h of aging time, decreases with decreasing film thickness for films less than ~100 nm thick. Additionally, the initial O<sub>2</sub>/N<sub>2</sub> selectivity increases as film thickness decreases, consistent with the permeability results. Superficially, these results appear to contradict reports of increased mobility near the surface of polymer films, since lower permeability and higher selectivity would typically be associated with decreased chain mobility. However, we believe the initially lower gas permeability in the ultrathin films is caused by aging occurring in the very first hour after the quench from above  $T_g$  (when it is not feasible to perform gas permeability measurements due to the time needed to prepare samples for study). If so, the enhanced mobility at the free surfaces allows ultrathin films to achieve a low free volume state (and, consequently, lower permeability and higher selectivity at one

hour, when permeability can first be measured) more quickly than bulk material [5]. This hypothesis is consistent with the results from the modelling study, which are described in more detail below.

### 3.3. Gas permeability and aging in Matrimid<sup>®</sup> films

The influence of aging time on oxygen, nitrogen, and methane gas permeability in Matrimid<sup>®</sup> films with thicknesses ranging from 550 nm down to 18 nm is presented in Fig. 6a, b, and c respectively. The aging response of these films is more pronounced than that of the PSF films with some films exhibiting a permeability decrease to ~30% of the original value after 1000 h of aging. The faster aging in Matrimid<sup>®</sup> as compared to PSF has been shown previously, and it is believed to result from the higher fractional free volume of Matrimid<sup>®</sup> relative to that of PSF [24]. Fig. 7a and b illustrate the impact of physical aging on the pure gas O<sub>2</sub>/N<sub>2</sub> and N<sub>2</sub>/CH<sub>4</sub> selectivity of Matrimid<sup>®</sup> films. Increasing selectivity with aging time is seen, as expected. Analogous to the PSF behavior, Matrimid<sup>®</sup> exhibits decreased permeability and increased selectivity at one hour of aging as film thickness is reduced. These differences are believed to

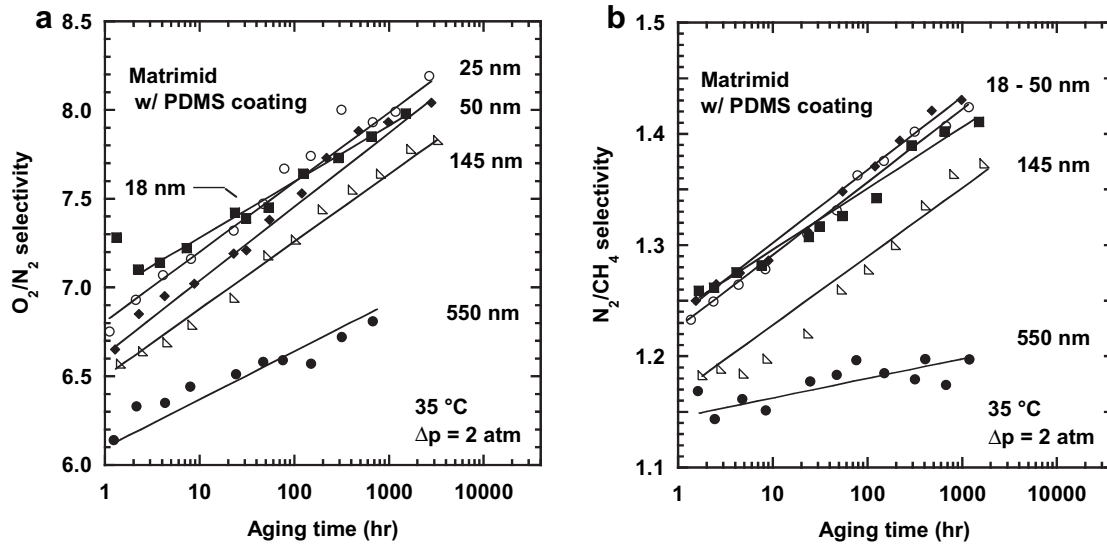


Fig. 7. Influence of physical aging on  $O_2/N_2$  pure gas selectivity (a) and  $N_2/CH_4$  pure gas selectivity (b) in Matrimid® films ranging from 550 nm to 18 nm in thickness as a function of aging time. Lines are provided to guide the eye.

be related to the physical aging that occurs in the first hour after the quench from above  $T_g$ .

### 3.4. Comparison to the upper bound

Robeson presented the trade-off between permeability and selectivity in polymer membranes, describing this relationship as the “upper bound” [37]. The theoretical basis for this relationship was later developed by Freeman [38]. Generally, this relationship describes the connection between permeability and selectivity in polymeric materials [39]. Fig. 8 shows the evolution of gas transport characteristics of the films studied, as a result of physical aging, relative to the upper bound. As the polymer ages, the trend of decreasing permeability and increasing selectivity move the film properties essentially parallel to the upper bound. The range of permeability and selectivity values exhibited by the same materials as a function of physical aging shows the significant effect prior history can have on gas transport properties of glassy polymers.

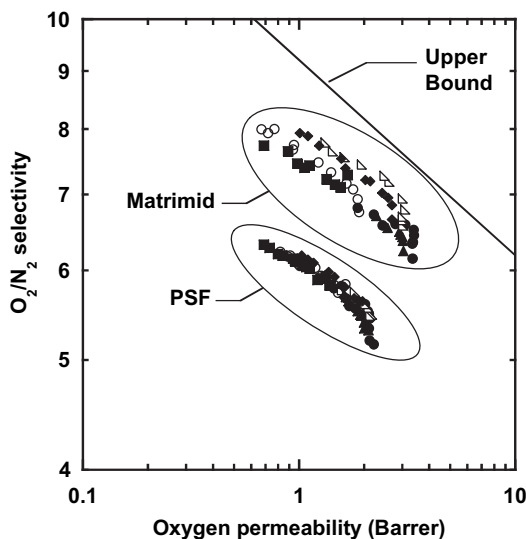


Fig. 8. Influence of physical aging in comparison with upper bound [36].

### 3.5. Modelling Considerations

The rate of physical aging, which is often modeled as shown in equation (2), depends on the ratio of the driving force, *i.e.*, the displacement of the specific volume from its equilibrium value, and the relaxation time for the sample, which is a function of temperature and the material’s current free volume state [18].

$$\text{Aging Rate} \equiv \frac{dv}{dt} = \frac{-(v - v_\infty)}{\tau(v, T_g - T)} \quad (2)$$

where  $v$  and  $v_\infty$  are the polymer specific volumes at time  $t$  and at equilibrium, respectively,  $T$  is temperature, and  $\tau$  is a characteristic relaxation time. Because the  $T_g$  in ultrathin PSF films is below the bulk value, as reported by Kim et al., these films should have enhanced mobility (*i.e.*, lower  $\tau$ ) as compared to the bulk [10]. Therefore, although ultrathin films may have a smaller departure from equilibrium (*i.e.*, a lower  $v - v_\infty$ ) than thicker films, as indicated by lower gas permeabilities and higher selectivities than thick films, enhanced chain mobility due to lower glass transition temperature in ultrathin films decreases the characteristic relaxation time (*i.e.*, decreases  $\tau$ ) [40]. The net effect of these two competing factors (*i.e.*, lower  $v - v_\infty$  and lower  $\tau$ ) on the rate of physical aging is to accelerate the physical aging response of these films, consistent with the experimental results shown in Figs. 4–7. While no report on the effect of film thickness on  $T_g$  in Matrimid®

Table 2  
Struik model parameters for PSF and Matrimid®.

Polymer	$\gamma$	$f_i$	$f_e$	$\tau_\infty$ (sec)	$\tau_\infty$ (sec)		
					$l$ (nm)	$O_2$	$N_2$
PSF	350	0.160	0.1069	465	$4.7 \times 10^{14}$	$1.8 \times 10^{14}$	$1.4 \times 10^{14}$
				125	$5.4 \times 10^{13}$	$1.8 \times 10^{13}$	$1.8 \times 10^{13}$
				75	$1.0 \times 10^{13}$	$3.2 \times 10^{12}$	$2.2 \times 10^{12}$
				50	$1.0 \times 10^{12}$	$4.0 \times 10^{11}$	$3.6 \times 10^{11}$
				20	$2.2 \times 10^{11}$	$1.1 \times 10^{11}$	$1.1 \times 10^{11}$
Matrimid®	200	0.176	0.1131	550	$3.5 \times 10^{11}$	$3.1 \times 10^{11}$	$2.6 \times 10^{11}$
				145	$5.2 \times 10^{10}$	$3.0 \times 10^{10}$	$1.8 \times 10^{10}$
				50	$6.8 \times 10^9$	$4.3 \times 10^9$	$2.2 \times 10^9$
				25	$5.0 \times 10^8$	$4.0 \times 10^8$	$2.5 \times 10^8$
				18	$2.2 \times 10^8$	$1.8 \times 10^8$	$1.1 \times 10^8$

**Table 3**  
Values for permeability correlation (equation (5)).

	O <sub>2</sub>		N <sub>2</sub>		CH <sub>4</sub>	
	A (Barrer)	B	A (Barrer)	B	A (Barrer)	B
Park & Paul [44]	397	0.839	112	0.914	114	0.967
PSF	397	0.839	125	0.914	210	0.967
Matrimid®	397	0.839	95	0.914	114	0.967

exists, the similarity in the permeability results suggest similar behavior could be expected.

To mathematically describe the influence of thickness-dependent relaxation times on physical aging-induced changes in permeability in ultrathin films, the self-retarding aging model developed by Struik to describe the variation in many physical properties (e.g., specific volume, impact strength, and creep compliance) of bulk glassy polymers with time is applied [18]:

$$\frac{d\Delta f}{dt} = \frac{-\Delta f}{\tau} = \frac{-\Delta f}{\tau_\infty \exp(-\gamma \Delta f)} \quad (3)$$

where  $\Delta f$  is the excess fractional free volume (i.e., the difference between the fractional free volume in the polymer,  $f$ , and the fractional free volume of the same material in the fully relaxed, equilibrium state,  $f_e$ ) (i.e.,  $\Delta f = f - f_e$ ),  $\tau$  is the relaxation time at time  $t$ ,  $\tau_\infty$  is the relaxation time at equilibrium (i.e., at  $t \rightarrow \infty$ ), and  $\gamma$  is a constant characterizing the sensitivity of the relaxation time to the excess fractional free volume. This model was developed for and validated using data from bulk polymers, where thickness effects on physical aging are not observed, so here  $\tau_\infty$  is allowed to depend on film thickness as a straightforward method to capture thickness-dependent aging behavior. The case of a thickness-dependent  $\gamma$  was also examined; however, the fit improvement did not justify allowing  $\gamma$  to depend on thickness, according to an  $F$ -test [41]. Free volume is related to the specific volume of the polymer,  $v$ , by

$$f = \frac{v - v_0}{v} \quad (4)$$

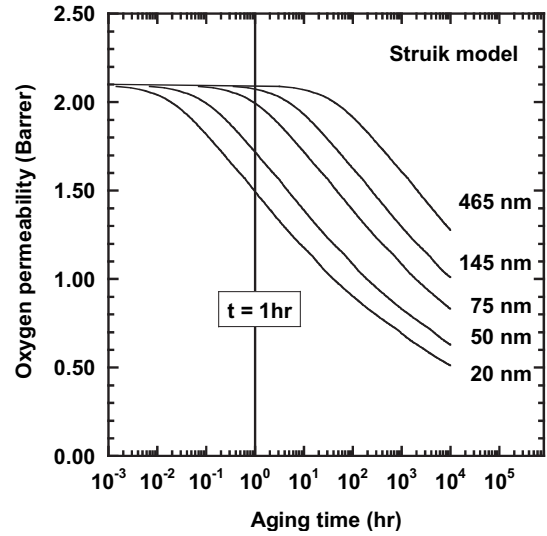


**Fig. 10.** Influence of aging time and film thickness on the predicted oxygen permeability behavior of the PSF films studied based on the modified Struik model.

where  $v_0$  is the occupied volume of the polymer (not needed in this analysis) which can be estimated by the Bondi method (i.e.,  $v_0 = 1.3v_w$ ), and  $v_w$  is the van der Waals volume estimated using the group contribution method [42]. The initial fractional free volume,  $f_i$ , used in the model was based on reported free volume values for PSF [34] and Matrimid® samples [43]. While the reported value of  $f_i$  for Matrimid® was determined for rapidly quenched thin film samples, the value for PSF was reported for bulk samples and required an increase from the reported 0.156 to 0.160 to account for the initially higher free volume in the rapid quenched state as compared to the bulk state. This change was based on matching the predicted initial O<sub>2</sub> permeability, using equation (5), with the experimental results for the bulk PSF films studied here. For both PSF and Matrimid®, the fractional free volume at the fully relaxed,

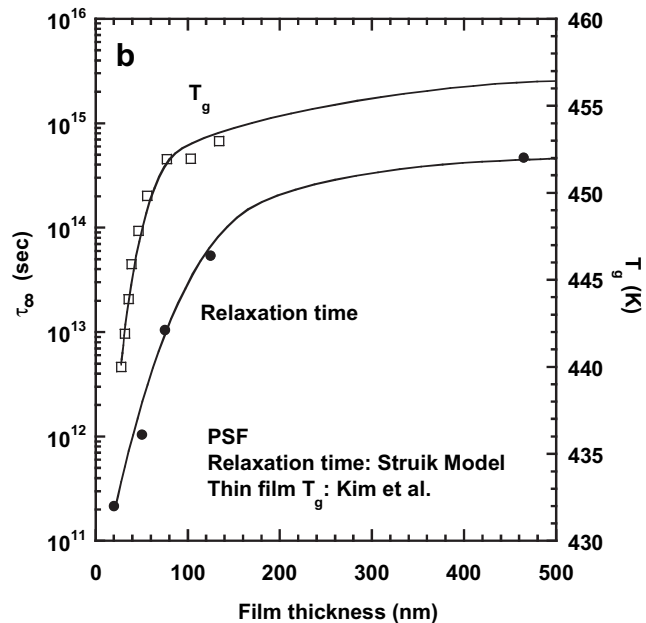
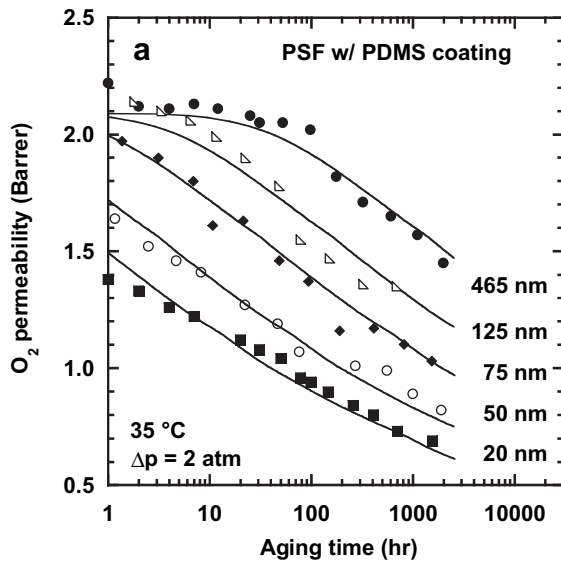


**Fig. 9.** The influence of film thickness on physical aging and relaxation rates. (a) Effect of aging time on oxygen permeability in PSF films ranging from 465 nm to 20 nm in thickness. Lines were generated from the modified Struik model. (b) Dependence of  $\tau_\infty$  (●) and  $T_g$  (□), from Kim et al.<sup>10</sup>, on PSF film thickness. The lines were drawn to guide the eye.

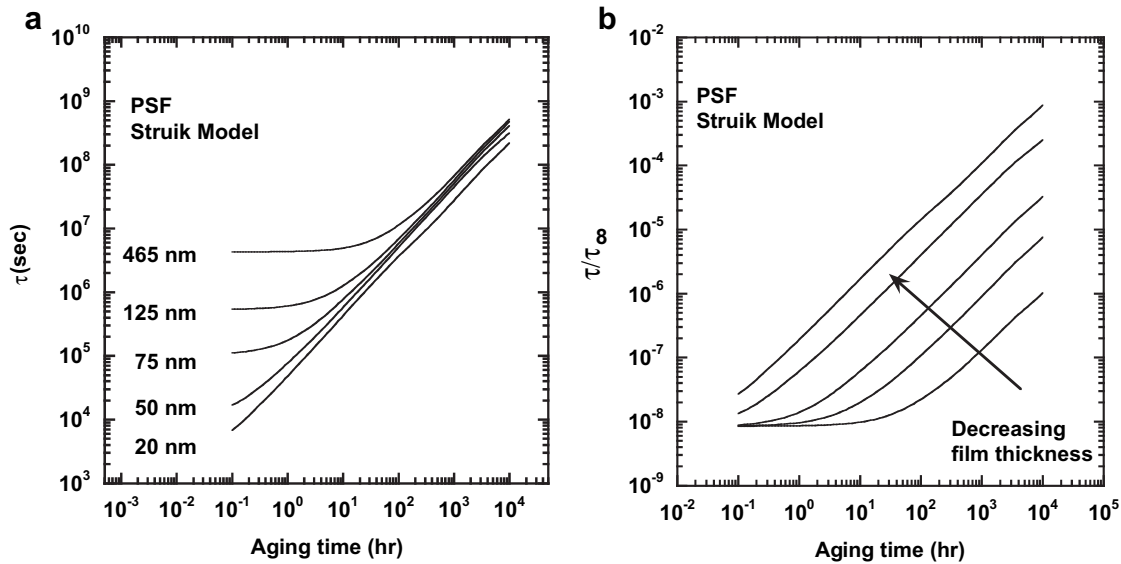


Fig. 11. Influence of aging time and film thickness on  $\tau$  (a), and the approach to the equilibrium relaxation time (b), based on the modified Struik model.

equilibrium state,  $f_e$ , was given by Huang et al. based on extrapolation of the experimental pressure-volume-temperature data in the melt state [43]. This aging model was solved numerically using MATLAB software. The fractional free volume,  $f$ , calculated as a function of aging time from equation (3) was used in the following correlation to calculate gas permeability:

$$P = Ae^{-B/f} \quad (5)$$

where  $A$  and  $B$  are constants based upon permeability measurements in samples of bulk thickness from the literature [44]. The permeability data were fit to the Struik model by allowing  $\tau_\infty$  and  $\gamma$  to vary to obtain the best fit in a least squares analysis.  $\gamma$  was not allowed to vary with film thickness, and  $\tau_\infty$  was allowed to depend on film thickness. The resulting Struik model parameters are shown in Table 2, while the  $A$  and  $B$  constants used in the permeability correlation are shown in Table 3. The combination of the correlation

in equation (5) and the thickness-dependent Struik model will be referred to hereafter as the modified Struik model.

### 3.6. Modelling PSF permeability and aging behavior

The modified Struik model, with only one thickness-dependent parameter,  $\tau_\infty$ , effectively captures the aging behavior of the ultrathin PSF films as shown in Fig. 9a. Fig. 9b illustrates the thickness dependence of  $\tau_\infty$  from the permeability results; this behavior suggests that accelerated aging in thinner films is achieved by the characteristic relaxation time decreasing by orders of magnitude as film thickness decreases. The relaxation times,  $\tau_\infty$ , deduced in this way show a remarkably similar trend with thickness as the reported thickness dependence of  $T_g$ , given by Kim et al. [10]. Apparently, the same mechanisms that appear to reduce  $T_g$  in ultrathin films contribute to accelerated aging in these materials by reducing the characteristic relaxation time as film thickness decreases [10].

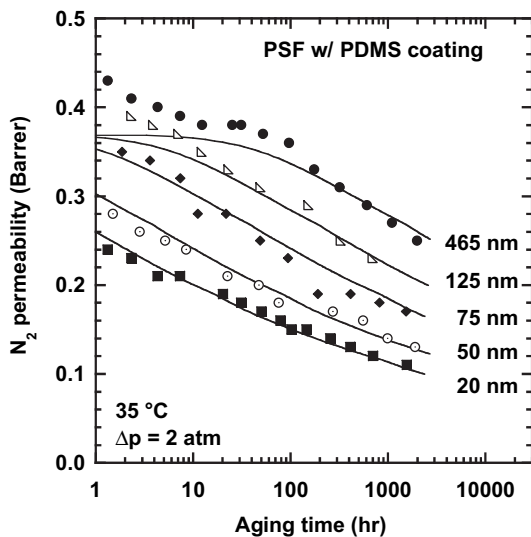


Fig. 12. Influence of aging time on nitrogen permeability in PSF films ranging from 465 nm to 20 nm in thickness. Lines were generated from the modified Struik model using the same relaxation times from the  $O_2$  modeling and  $A = 112$  Barrer for  $N_2$ .

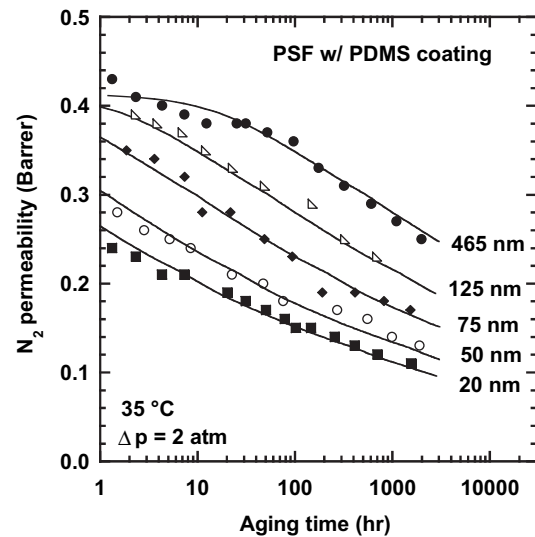


Fig. 13. Influence of aging time on nitrogen permeability in PSF films ranging from 465 nm to 20 nm in thickness. Lines were generated from the modified Struik model using  $A = 125$  Barrer for  $N_2$ .



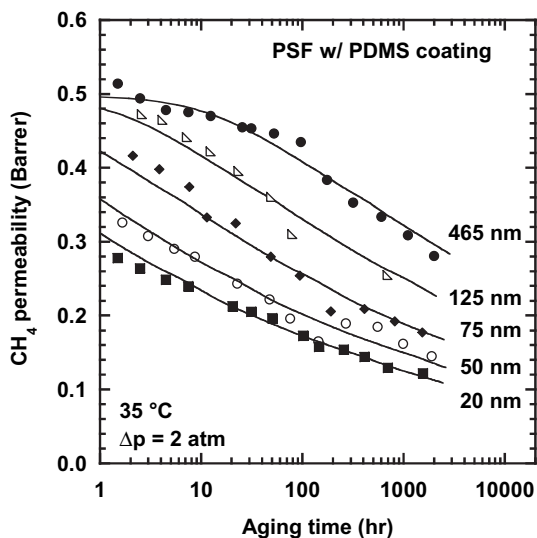


Fig. 14. Influence of aging time on methane permeability in PSF films ranging from 465 nm to 20 nm in thickness. Lines were generated from the modified Struik model.

Fig. 10 presents the predicted  $O_2$  permeability behavior of the PSF films studied including times  $\ll 1$  h. By changing only  $\tau_\infty$  with film thickness, the initial conditions of each film are identical, i.e., at very short times following the thermal quench, all films have the same permeability. The vertical line drawn at 1 h of aging is included to illustrate why the initial permeability measured experimentally (i.e., permeability at one hour, when it first becomes possible to measure permeability) decreases with decreasing film thickness.

The values of  $\tau$  as a function of film thickness and aging time are shown in Fig. 11a. In all films,  $\tau$  increases with aging time in this self-retarding model whereby aging slows as it progresses. It is interesting to note that at short aging times the difference in  $\tau$  between the films studied spans several orders of magnitude, but after  $\sim 1000$  h of aging, this difference is less than one order of magnitude. Fig. 11b illustrates the approach to  $\tau_\infty$  as a function of film thickness, demonstrating how the thin films approach equilibrium more rapidly than the thicker films. Once the reduced relaxation time, i.e.,  $\tau/\tau_\infty$ , begins to increase linearly with log aging time, the slope of the approach to unity is the same for each film thickness because the model parameters are the same for each case, except for the equilibrium relaxation time. This approach shows that each film ages similarly, and results in simply shifting the aging curve as a function of film thickness.

The same model parameters which describe the oxygen permeability data in PSF can also be used to estimate to the nitrogen permeability data by applying the appropriate values of  $A$  and  $B$  in equation (4). The results of this analysis, using the Struik model parameters from the  $O_2$  modelling and literature values of  $A$  and  $B$  for  $N_2$ , are shown in Fig. 12. While the model does a fair job of capturing the experimental data, there is some disagreement at early aging times in the thicker films. This discrepancy is believed to be related to the initial molecular relaxations that affect the larger  $N_2$  molecules more than the  $O_2$  molecules. All glassy polymers will have a distribution of free volume element sizes, with the average size being considered in the Struik model. However, according to the Struik model, larger free volume sites (i.e., those large enough to accommodate either  $N_2$  or  $O_2$ ) age more rapidly than smaller free volume sites (i.e., those large enough only to accommodate  $O_2$ ) due to their inherently greater displacement from the equilibrium state. By allowing  $\tau_\infty$  to change from gas to gas, an improved fit of the

nitrogen permeability aging data is achieved, shown in Fig. 13a. It was also necessary to adjust the  $A$  parameter from 112 (i.e., the literature value [44]) to 125 Barrer to match the initial  $N_2$  permeability in the PSF films. Although the literature values of  $A$  and  $B$  used in equation (4) generally predict permeability well, some changes in  $A$  were required to better match the behavior of the specific polymers considered here. Some adjustment of these parameters is expected to closely match the behavior of individual polymers. The intent here is not to make parameter adjustments tailored to the data; rather, it is to provide a qualitative analysis of the underlying physical phenomena related to aging. The  $\tau_\infty$  values used to calculate the  $O_2$  and  $N_2$  permeability of the 465 nm film are shown in Table 2. The shorter relaxation time for the  $N_2$  permeability behavior indicates that the rate of relaxation of the free volume which affects  $N_2$  permeability is greater than for  $O_2$  permeability, in qualitative agreement with the expectation from the Struik model (i.e., that larger free volume elements age faster).

Fig. 14 compares the methane permeability behavior to predictions from the modified Struik model. For  $CH_4$ , the relaxation times were similar to those used for  $N_2$ , seen in Table 2. Also, the value for  $A$  in the permeability correlation was changed from 114 (i.e., the literature value [44]) to 210 Barrer to better match the  $CH_4$  permeability in PSF.

### 3.7. Modelling Matrimid<sup>®</sup> permeability and aging behavior

The modified Struik model was also applied to describe the Matrimid<sup>®</sup> permeability data. Fig. 15a, b, and c show the close agreement between the model and the oxygen, nitrogen, and methane permeability behavior. The parameters used in the modified Struik model are shown in Table 2. The values used in the permeability correlations for Matrimid<sup>®</sup> were the same as those reported by Park and Paul[44], except the  $A$  value for  $N_2$ , which was changed from 112 to 95 Barrer, as shown in Table 3. The  $\tau_\infty$  values for the larger gases (i.e.,  $N_2$  and  $CH_4$ ) are somewhat smaller than that of the smaller gas,  $O_2$ , consistent with the results observed in PSF. The relaxation times for the Matrimid<sup>®</sup> films are shorter than for the PSF films, consistent with faster aging in Matrimid<sup>®</sup>.

The lower value of  $\gamma$  in Matrimid<sup>®</sup>, as compared to PSF, indicates a weaker influence of free volume on the aging rate in Matrimid<sup>®</sup> than in PSF. The influence of free volume on local chain mobility important for physical aging can be expected to vary from one material to another. Crudely speaking, one might imagine two extreme cases, one being the situation where the limiting factor for such local motion is the energy required to overcome energy barriers between covalently connected moieties along the chain backbone (i.e., the barrier to chain motion is entirely due to intramolecular restrictions on chain segment motion) and the second being the case where the limiting factor is the energy required to move neighboring chain segments out of the way so that aging-related local motion can occur (i.e., the barrier to chain motion is entirely due to intermolecular restrictions on chain motion). Free volume should predominantly influence chain packing and, in turn, intermolecular energy barriers, but not the energy barriers between covalent linkages along a given chain. Therefore, in the first case, one would expect little to no effect of free volume on the timescale of molecular motion (i.e., low values of  $\gamma$ ), and in the second case, one would expect a maximum effect of free volume on the timescale for molecular motion (i.e., high values of  $\gamma$ ). Thus, the experimental result that  $\gamma$  is higher in PSF than in Matrimid<sup>®</sup> suggests that intra-molecular mobility restrictions, such as that due to a rigid chain structure, are more influential in Matrimid<sup>®</sup> than PSF, which is consistent with the considerably higher  $T_g$  value of Matrimid<sup>®</sup> relative to PSF. Interestingly, this result of the more rigid, higher  $T_g$  polymer exhibiting faster relaxation is reminiscent

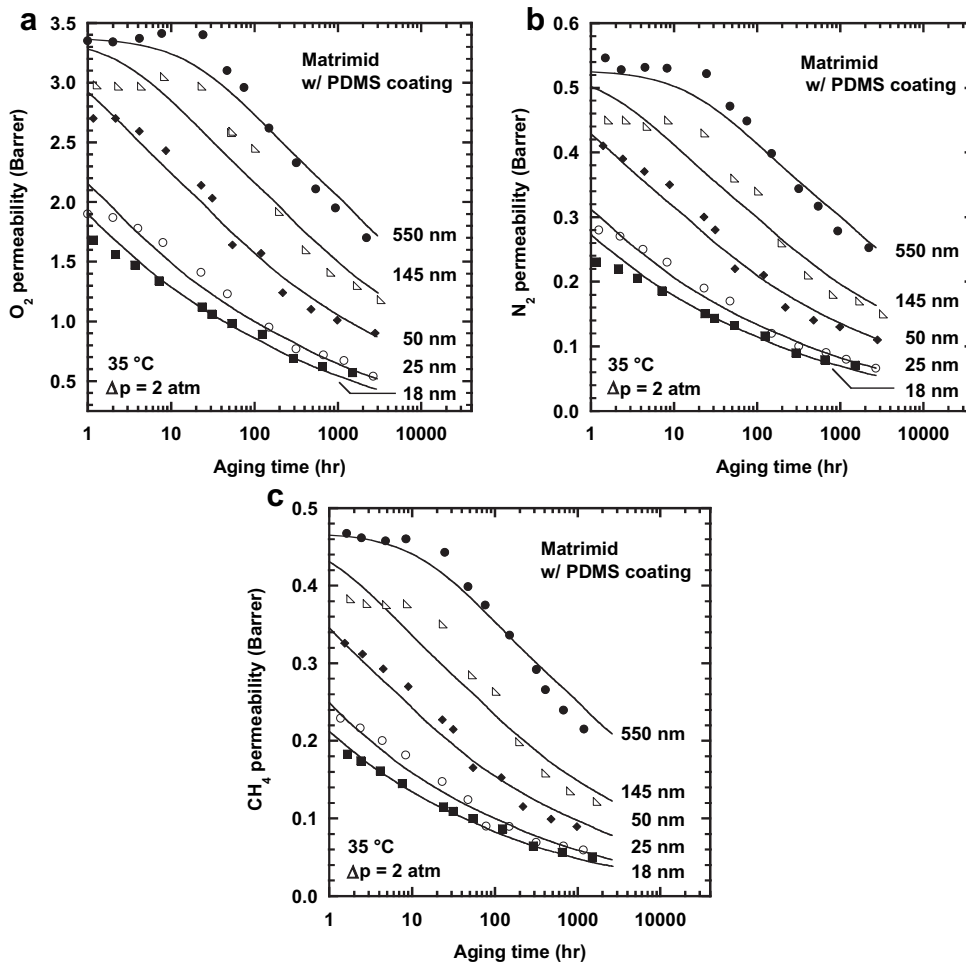


Fig. 15. Influence of physical aging on oxygen permeability (a), nitrogen permeability (b), and methane permeability (c) in Matrimid® films ranging from 550 nm to 18 nm in thickness. Lines were generated from the modified Struik model using gas-specific parameters shown in Tables 2 and 3.

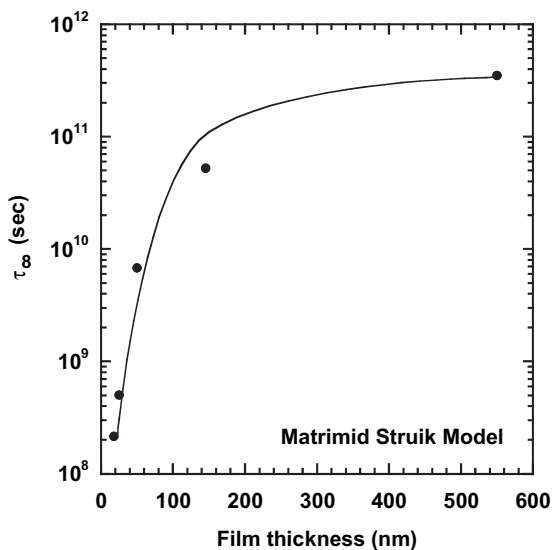


Fig. 16. Influence of film thickness on  $\tau_{\infty}$  in modeling the oxygen permeability of Matrimid® films based on the modified Struik model. The line is drawn to guide the eye.

of the influence of structural symmetry on polymer behavior. For example, polysulfones with para linkages across phenol rings in the main chain consistently have higher  $T_g$  and yet higher mobility, as related to penetrant diffusion, as compared to their meta linked analogs [45].

The influence of film thickness on  $\tau_{\infty}$  in Matrimid® according to the modified Struik model is shown in Fig. 16. As seen in PSF,  $\tau_{\infty}$  decreases by several orders of magnitude as film thickness is reduced. For the other gases studied, film thickness had similar influences on  $\tau_{\infty}$ , i.e., as film thickness decreases,  $\tau_{\infty}$  decreases.

#### 4. Conclusions

Understanding the influence of nanoscale confinement on physical aging, or structural relaxation, is essential for describing glassy dynamics of confined polymer systems and for predicting the long-term performance of glassy materials in a variety of technologies, including gas separation membranes. Enabled by a newly applied coating technique, the gas permeability and physical aging of PSF and Matrimid® films as thin as 18 nm thick were studied. All films exhibited rapidly decreasing permeability and increasing selectivity with aging time. Additionally, the initial permeability, measured at one hour of aging, of the ultrathin films decreased with decreasing film thickness. Analysis of the permeability/selectivity characteristics exhibited during aging, compared with the upper

bound, shows the sensitivity of gas transport properties to previous history. The greatly accelerated aging in ultrathin films, as compared to bulk behavior, is consistent with the notion of enhanced mobility at the polymer surface, which is the same mechanism thought to cause  $T_g$  reductions in ultrathin films. Struik's physical aging model can capture the observed trends in permeability aging if the characteristic relaxation time is allowed to vary with thickness. Small model parameter adjustments lead to a more accurate description of the behavior of different gases; the results of these changes are consistent with the model whereby larger free volume elements age more rapidly than smaller elements.

## Acknowledgements

This research was supported by Air Liquide/MEDAL, the National Science Foundation (Grant DMR 238979 administered by the Division of Material Research – Polymer Program), and the NSF Science and Technology Center for Layered Polymeric Systems (Grant DMR-0423914).

## References

- [1] Bitá I, Yang JKW, Jung YS, Ross CA, Thomas EL, Berggren KK. *Science* 2008; 321(5891):939–43.
- [2] Brauman JI, Szuromi P. *Science* 1996;273(5277):855.
- [3] Forrest JA, Dalnoki-Veress K. *Advances in Colloid and Interface Science* 2001;94(1–3):167–95.
- [4] Frank CW, Rao V, Despotopoulou MM, Pease RFW, Hinsberg WD, Miller RD, et al. *Science* 1996;273(5277):912–5.
- [5] Jerome B, Commaudeur J. *Nature* 1997;386(6625):589–92.
- [6] Ruiz R, Kang H, Detcheverry FA, Dobisz E, Kercher DS, Albrecht TR, et al. *Science* 2008;321(5891):936–9.
- [7] Ibn-Elhaj M, Schadt M. *Nature* 2001;410(6830):796–9.
- [8] Jones RL, Kumar SK, Ho DL, Briber RM, Russell TP. *Nature* 1999;400(6740):146–9.
- [9] Ellison CJ, Kim SD, Hall DB, Torkelson JM. *The European Physical Journal E – Soft Matter* 2002;V8(2):155–66.
- [10] Kim JH, Jang J, Zin WC. *Langmuir* 2000;16(9):4064–7.
- [11] Serghei A, Huth H, Schick C, Kremer F. *Macromolecules* 2008;41(10):3636–9.
- [12] Serghei A, Mikhailova Y, Eichhorn KJ, Voit B, Kremer F. *Journal of Polymer Science Part B Polymer Physics* 2006;44(20):3006–10.
- [13] Ellison CJ, Torkelson JM. *Nature Materials* 2003;2(10):695–700.
- [14] Fakhraai Z, Valadkhan S, Forrest J. *The European Physical Journal E – Soft Matter* 2005;18(2):143–8.
- [15] Priestley RD, Ellison CJ, Broadbelt LJ, Torkelson JM. *Science* 2005;309(5733):456–9.
- [16] Kawana S, Jones RAL. *European Physical Journal E Soft Matter* 2003;10(3):223–30.
- [17] Simon SL, Park JY, McKenna GB. *The European Physical Journal E – Soft Matter* 2002;8(2):209–16.
- [18] Struik LCE. *Physical aging in amorphous polymers and other materials*. Amsterdam: Elsevier; 1978.
- [19] Hutchinson JM. *Progress in Polymer Science* 1995;20(4):703–60.
- [20] Kurchan J. *Nature* 2005;433(7023):222–5.
- [21] Hickner MA, Ghassemi H, Kim YS, Einsla BR, McGrath JE. *Chemical Reviews* 2004;104(10):4587–612.
- [22] Halls JJM, Walsh CA, Greenham NC, Marseglia EA, Friend RH, Moratti SC, et al. *Nature* 1995;376(6540):498–500.
- [23] Baker RW. *Industrial and Engineering Chemistry Research* 2002;41(6):1393–411.
- [24] Huang Y, Paul DR. *Polymer* 2004;45(25):8377–93.
- [25] Priestley RD, Broadbelt LJ, Torkelson JM. *Macromolecules* 2005;38(3):654–7.
- [26] Pinnau I, Koros WJ. *Journal of Applied Polymer Science* 1991;43(8):1491–502.
- [27] McCaig MS, Paul DR. *Polymer* 2000;41(2):629–37.
- [28] Pfromm PH, Koros WJ. *Polymeric Materials Science and Engineering* 1994;71:401–2.
- [29] Dorkenoo KD, Pfromm PH. *Macromolecules* 2000;33(10):3747–51.
- [30] Henis JMS, Tripodi MK. *Science* 1983;220(4592):11–7.
- [31] Henis JMS, Tripodi MK. *Separation Science and Technology* 1980;15(4):1059–68.
- [32] Koros WJ, Paul DR, Rocha AA. *Journal of Polymer Science Polymer Physics Edition* 1976;14(4):687–702.
- [33] Henis JMS, Tripodi MK. *Journal of Membrane Science* 1981;8(3):233–46.
- [34] McHattie JS, Koros WJ, Paul DR. *Polymer* 1991;32(5):840–50.
- [35] Merkel TC, Bondar VI, Nagai K, Freeman BD, Pinnau I. *Journal of Polymer Science Part B Polymer Physics* 2000;38(3):415–34.
- [36] Ensore DJ, Hopfenberg HB, Stannett VT, Berens AR. *Polymer* 1977;18(11):1105–10.
- [37] Robeson LM. *Journal of Membrane Science* 1991;62(2):165–85.
- [38] Freeman BD. *Macromolecules* 1999;32(2):375–80.
- [39] Robeson LM. *Journal of Membrane Science* 2008;320(1–2):390–400.
- [40] Koh YP, Simon SL. *Journal of Polymer Science Part B Polymer Physics* 2008;46(24):2741–53.
- [41] Bevington PR, Robinson DK. *Data reduction and error analysis for the physical sciences*. 2nd ed. New York: McGraw–Hill, Inc.; 1992.
- [42] Krevelen DWV. *Properties of polymers*. 3rd ed. Amsterdam: Elsevier; 1990.
- [43] Huang Y, Wang X, Paul DR. *Journal of Membrane Science* 2006;277(1–2):219–29.
- [44] Park JY, Paul DR. *Journal of Membrane Science* 1997;125(1):23–39.
- [45] Aitken CL, Koros WJ, Paul DR. *Macromolecules* 1992;25(13):3424–34.